Acoustic tomography in the atmospheric surface layer

Astrid Ziemann, Klaus Arnold, Armin Raabe

Zusammenfassung:

Die vorgestellte Methode der akustischen Tomographie (Simultane Iterative Rekonstruktionstechnik) und ein spezieller Auswertungsalgorithmus können flächengemittelte Werte meteorologischer Größen direkt bereitstellen. Somit werden zur Validierung numerischer mikroskaliger Atmosphärenmodelle weitgehend konsistente Daten geliefert.
Das Verfahren verwendet die horizontale Ausbreitung von Schallstrahlen in der atmosphärischen Bodenschicht. Um einen allgemeinen Überblick zur Schallausbreitung unter verschiedenen atmosphärischen Bedingungen zu erhalten, wird ein zweidimensionales Schallausbreitungsmodell genutzt.
Von Messungen der akustischen Laufzeit zwischen Sendern und Empfängern an verschiedenen Punkten in einem Meßfeld kann der Zustand der durchquerten Atmosphäre abgeschätzt werden. Die Ableitung flächengemittelter Werte für die Schallgeschwindigkeit und der daraus deduzierten Lufttemperatur resultiert aus der Inversion der Laufzeitwerte für alle möglichen Schallwege. Das angewandte zweidimensionale Tomographiemodell mit geradliniger Schallstrahlapproximation stellt dabei geringe Computeranforderungen und ist auch während des online-Betriebes einfach zu handhaben.

Summary:

The presented method of acoustic tomography (Simultaneous Iterative Reconstruction Technique) and a special algorithm of analysis can directly provide area averaged values of meteorological quantities. As a result rather consistent data will be delivered for validation of numerical atmospheric micro-scale models.
The procedure uses the horizontal propagation of sound waves in the atmospheric surface layer. To obtain a general overview of the sound propagation under various atmospheric conditions a two-dimensional ray-tracing model is used.
The state of the crossed atmosphere can be estimated from measurements of acoustic travel time between sources and receivers on different points in an tomographic array. Derivation of area averaged values of the sound speed and furthermore of air temperature results from the inversion of travel time values for all possible acoustic paths. Thereby, the applied straight-ray two-dimensional tomographic model is characterised as a method with small computational requirements and simple handling, especially, during online working.

1. Introduction

The development of micro-scale atmospheric and LES (Large Eddy Simulation) models which are applied for different questions in meteorology, forces their validation by means of accurate experimental data and so the derivation of area averaged meteorological quantities.
Spatial averaged data and so consistent data for model validation were conventionally provided by point measurements and a following interpolation technique. A relatively new way to get

such values directly is the transfer of tomographic methods to the atmospheric surface layer (see Spiesberger and Fristrup, 1990; Wilson and Thomson, 1994).
As an inverse technique tomography has been used routinely for instance in medicine, biology, geophysics and oceanography for many years (see, e.g., Munk et al., 1995).
There are various advances of tomographic measurements compared with conventional methods, e.g., the effect as spatial filter for turbulence below the micro-scale, the remote monitoring, because the test medium is not influenced by devices, the higher number of data per sensor in comparison to the traditional point measurements (Wilson and Thomson, 1994).
In our study we use a kind of acoustic travel time tomography, where the sound speed can be determined by measuring the travel time of a signal at a defined propagation path. Applying a suitable procedure measurements of the speed of sound can be used to reconstruct the spatially and temporally variable temperature and wind fields.
Wilson and Thomson (1994) demonstrated the applicability of acoustic tomography to the atmospheric boundary layer. The significant difference to the work presented here lies in the numerical algorithm used and in the kind of the output. We exert the tomographic technique SIRT (Simultaneous Iterative Reconstruction Technique) to provide from the measured line integrals, the travel time data, not only differences from a mean value, but also area averaged absolute values for the sound speed and the air temperature, respectively. Our measuring system, which can be used for a wide range of environmental and equipment situations, is introduced as a method to complete meteorological point measurements, especially, during experimental campaigns.
The following chapter describes some fundamentals of the sound propagation in the atmosphere. In chapter 3, a general review of the tomographic methods and, especially, of the SIRT used in our study is given. The next chapter deals with the implementation of the presented principles of geometric acoustics and tomography in numerical models, namely a two-dimensional ray-tracing model for a stratified atmosphere and a tomographic model according to a horizontal-slice scheme. In chapter 5, the experimental equipment and the processing of acoustic signals as well as the demanded accuracy of the travel time data are described. Finally, in chapters 6 and 7 results of our last experimental campaign MEPEX'97 in autumn 1997 and an outlook to necessary improvements are supplied.

2. Theoretical bases of the sound propagation in the atmosphere

In addition to the well-known reduction of the sound level with increasing distance from the sound source the damping due to the influence of inhomogeneities within the atmosphere, the structure of the ground and the air absorption play a role during the sound propagation through the atmosphere. If the sound propagation can be considered as spreading of small perturbations in an unbounded, frictionless and compressible fluid without external forces the wave equations

$$\frac{\partial^2 \rho'}{\partial t^2} = c^2 \Delta \rho' \text{ and } \frac{\partial^2 p'}{\partial t^2} = c^2 \Delta p' \qquad \left(\Delta = \nabla^2 \text{ as usual}\right) \tag{1}$$

can be obtained from the Euler equation and the continuity equation with the well-known relationship between the pressure, p, and the air density, ρ, fluctuations, $p' = c^2 \rho'$, and between the sound speed and the compressibility, $c^2 = \frac{dp}{d\rho}$ (see, e.g., Birkhoff, 1988; Pierce, 1989; Spiesberger and Fristrup, 1990).

If the dry air is considered as an ideal gas, Laplace's equation of sound speed can be used under adiabatic conditions:

$$c = \sqrt{\kappa R_a T}, \tag{2}$$

where T is the air temperature in Kelvin, R_a $\left(= 287.05 \text{ J kg}^{-1} \text{ K}^{-1}\right)$ is the dry adiabatic gaseous constant and κ $(= 1.4)$ is the compressibility.

Effects of air humidity (e.g., Spiesberger and Fristrup, 1990) or a modified air composition on sound velocity are neglected because typical changes are less than 0.05%.

Additionally to spatial (x, y, z) and temporal (t) alterations concerning changes of air temperature, also an influence in consequence of the wind field $\vec{v}(t,x,y,z)$ appends to the sound velocity and leads to an effective sound speed vector using the approximation of wave fronts from geometrical acoustics (see Pierce, 1989) with $\vec{n}$ as unit vector normal to the wave front:

$$\vec{c}_{eff}(T,\vec{v}) = c(T(t,x,y,z))\vec{n}(t,x,y,z) + \vec{v}(t,x,y,z) \tag{3}$$

Thereby, the conditions for sound propagation are changed and so a deviation from straightforward course between sound sources and receivers can be observed.

The sound propagation can be described with sound rays if the principles of the geometric acoustics, i.e., small acoustic refraction index gradient compared to the wave number of the sound wave (e.g., Klug, 1991), are applicable. This case often occurs under outdoor conditions except in the direct vicinity of the ground. Then sound rays represent lines whose tangents correspond to the propagation direction of the sound wave. Although the use of the sound ray theory, which is based on the principles of Fermat and Huygens, is associated with limitations, it offers, in comparison to wave models, the following advantages: (1) an easy visualisation of sound propagation inside the atmosphere and (2) a simple consideration of inhomogeneities inside the medium by application of the refraction law.

At the boundary between two parts of the atmosphere, which are characterised by different values of air temperature and wind vector the sound rays are refracted. This refraction is due to a variation in air temperature and wind vector depending on altitude in stratified fluids. According to Fasold et al. (1984) we used a general form of Snell's law for a moving and vertical inhomogeneous medium with the same frequency f in the two layers 1 and 2:

$$\sin\alpha_2 = \frac{k_1 \sin\alpha_1}{k_2 + (k_2|\vec{Ma}_1|\cos\varphi - k_1|\vec{Ma}_2|\cos\varphi)\sin\alpha_1} \tag{4}$$

$$\text{with} \quad |\vec{Ma}_1| = \frac{|\vec{v}_1|}{c_2}, \; |\vec{Ma}_2| = \frac{|\vec{v}_2|}{c_1}, \; k_1 = 2\cdot\pi\cdot\frac{f}{c_1}, \; k_2 = 2\cdot\pi\cdot\frac{f}{c_2}$$

Thereby, α_1 is the incident and α_2 is the refracting angle, φ is the angle between the wind direction and the undisturbed (without wind influence) sound velocity vector, Ma_1 and Ma_2 are the Mach numbers, k_1 and k_2 are the wave numbers. Note that the angles α_1 and α_2 are related to the wave normals in the layers 1 and 2, respectively.

According to numerous authors (Tatarskii, 1961; Kneser, 1961; Aubry et al., 1974; Daigle et al., 1978; Bass, 1981), other atmospheric influences, like the changes of the sound pressure level caused by scattering of the sound waves on temperature inhomogeneities and turbulence elements as well as the damping in consideration of air absorption, can be neglected for the frequency range used here, namely 1000 Hz, and source-receiver distances between 50 and 300 m.

However, the influence of the soil and the land cover can be much greater. After many authors (Embleton et al., 1976; Chessel, 1977; Bolen et al., 1981; Rasmussen, 1986; Klug, 1991; Salomons, 1994) a minimum in the transfer function, i.e., the sound pressure level related to undisturbed conditions of propagation, can occur near a frequency of about 500 Hz for grassland. Such damping due to sound wave interference increases with the distance between the source and the receiver and also with decreasing height of the experimental tools above the reflecting plane. According to Klug (1991), the described ground dip disappears by positive gradients of the sound velocity, by an increasing turbulent exchange or by use of a changed measuring geometry with device heights greater than 4 m as well as higher frequencies.

3. Travel time tomography

The theoretical basis of tomography lies on the Radon transformation (Radon, 1917) related to the projection of a two-dimensional scalar field and the transition from the measured value distribution to the projection field. According to Radon's law, it is possible to reconstruct a spatial distribution of parameters by inversion of line integral values, e.g., measured travel times. That means, that a continuously two-dimensional function can be derived from an infinite number of its continuously one-dimensional projections. The task is to determine the original distribution of parameter values from the measured projections. Thereby, the projection-slice scheme will be applied (e.g., Rüter and Gelbke, 1986).
The general principle of tomography (Greek 'tomos' means slice or section), as a certain image reconstruction technique and solving method for inversion problems, is to create a model of physical parameters in such a way that the projected data agree with the measured data.
Review of first applications of acoustic tomography is given by Wilson and Thomson (1994). The historical development, especially, in seismic applications of tomography is presented at Humphreys and Clayton (1988). Recently tomographic methods of the sound propagation in the atmosphere were applied by Spiesberger and Fristrup (1990) who described a method for passive localisation of calling animals and by Wilson and Thomson (1994) who primarily include the characterisation of the atmosphere. The main differences of these works to our study exist in the experimental design, the signal processing and the interpretation algorithm including the tomographic method. Both the studies, the presented here and the one from Wilson and Thomson (1994), use horizontal-slice schemes, i.e., a two-dimensional tomography. The advantages of our procedure are the small computational time and memory requirements. Only one ray is in the memory at one time. Therefore, it is possible to use the introduced model also for online interpretation of measuring results during experimental studies.
According to Worthington (1984), the procedures to solve tomographic problems can be divided into three main groups. Direct analytical solutions based on Fourier or inverse Radon transformation are usually employed for biological and medical applications with a homogenous ray covering of a high density. Alternative methods were developed, e.g., in geophysics and oceanography, where such ideal ray and angle covering usually does not occur.
One possible algorithm to solve the linear equation system with the desired parameter values as unknown variables is the matrix inversion method. Thereby, the generalised matrix inversion is the most important procedure if there are more unknowns than linearly independent equations (see Aki and Richards, 1980; Backus and Gilbert, 1968). Because of the very space- and time-consuming handling of large matrixes, which have to be inverted, the practical applicability of this method is limited. Furthermore, significant stability problems can occur during inversion (Krajewski et al., 1989). Consequently, methods referred to as row action (Trampert and

Leveque, 1990) or ART (Algebraic reconstruction Technique), in which the approximate solution is updated by successively processing the equations, are more attractive.
The large number of iterative reconstruction techniques (e.g., Peterson et al., 1985) can successfully be used for different measurement geometries with irregular sampling or limited projection angles with the additional advantage of simple handling and small computational requirements. The most prominent methods are the ART and the SIRT according to Gordon et al. (1970) and Gilbert (1972), respectively. A comprehensive review of to the mathematical background of ART-like methods is given by van der Sluis and van der Vorst (1987). Techniques, which update the approximate solution only after all equations have been processed, are called SIRT (Trampert and Leveque, 1990). In our study we apply a special form of this method.
Principally, an observed data set consists of line integrals along a specified path of the parameter to be imaged, e.g., acoustic travel time, which contains information about the physical quantities of the medium. Inhomogeneities of air temperature or in the wind field inside the tomographic array influence each measured travel time in an other way. Each measurement is ambiguous, only the inversion of every travel time measurement produces an image of the medium features radiated through with sound rays.
For a two-dimensional consideration the line integral for the travel time τ of a signal between a fixed acoustic source and receiver can be acquired

$$\tau = \int_{ray} \frac{dl}{|\vec{c}_{eff}|(t,x,y)} = \int_{ray} s(t,x,y)dl, \qquad (5)$$

where dl is the element of arc length along the propagation path and s symbolises the slowness, i.e., the reciprocal effective sound velocity.
Fundamental difficulties thereby are that the ray path itself depends on the unknown slowness distribution and that therefore the line integral becomes non-linear in slowness. Usually, a linearisation is applied to get some initial slowness model and to solve this problem. Thereby, straight lines connecting the sound source and the receiver are used to approximate the true ray path.
In the praxis only a limited number of measurements is available. Therefore, the searched two-dimensional function can only be reconstructed as a discrete parameter distribution, i.e., constant parameter values inside the grid cells. Various discretizations are possible. We use a tomographic array covered with square cells of constant size. The linearized set of equations in discrete form follows that of Rüter and Gelbke (1986) as

$$\tau_i = \sum_{j=1}^{J} s_j l_{ij} \qquad \text{with} \qquad s_j = \frac{1}{c_j}, \qquad (6)$$

where τ_i is the travel time of the i^{th} sound ray, s_j and c_j are the slowness and the effective sound speed in grid cell j, respectively, and l_{ij} is the length of the ray piece of the ray i in the j^{th} cell.
An image of diverse properties of the domain, which were radiated through from several angles of view, can be deduced by the following inversion technique. Thereby, the measuring field (260×200 m^2) of our experimental campaign MEPEX'97 was divided into small area elements (20×20 m^2) according to Fig. 1.
The dimension of the grid cells was chosen depending on the number of sound rays and the wished resolution. For each grid cell constant values of the slowness and the sound speed, respectively, were assumed.
In the mean travel time τ_i an information about the searched travel time and slowness in each grid cell j can be extracted using the known ray path l_{ij}. The aim of the following procedure is the reconstruction of the slowness s_j.

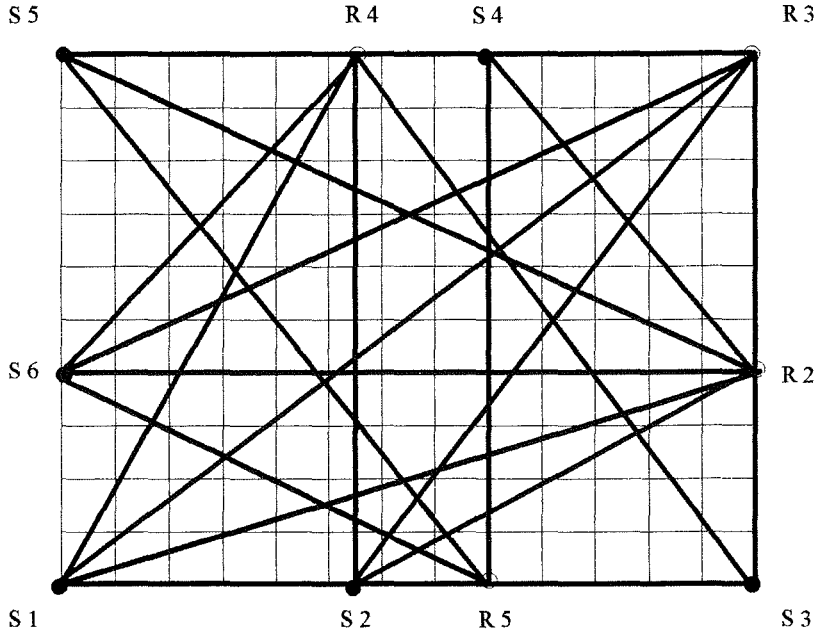

Fig. 1. Layout of the tomographic array (200 × 260 m²). The grid cells (20 × 20 m²) symbolise the solution of the tomographic model. The sources are labeled S1 to S6, the receivers are labeled R2 to R5. Note that R1 is the frequency generator.

In our study we applied a kind of straight ray tomography, the simplest ray tracing between sources and receivers. The error made by this approximation is investigated with a ray tracing model which requires high resolved vertical profiles of meteorological quantities. This model is described in chapter 2 and 4.

For every algebraic reconstruction technique a forward model has to be proposed in order to get the searched distribution by an iterative comparison process between calculated and experimental data. Starting with an initial guess of the slowness values, s_i^0, SIRT iterates on the difference between the experimental obtained travel time $\tau_i^{measure}$ and the last model prediction τ_i. After back projection of this difference and adding the resulting correction $\bar{k}_j$ to the present model an updated version of the simulated travel time follows. Thereby, corrections $\bar{k}_j$ are carried out to meet the condition:

$$\tau_i^{measure} = \sum_{j=1}^{J} (s_j + \bar{k}_j) x_{ij} \tag{7}$$

Among all grid cells an averaged value for correction $\bar{k}_j$ will be obtained from the distribution of the differences

$$\Delta\tau_i = \tau_i^{measure} - \tau_i \tag{8}$$

This corresponds to the minimum energy criterion, after multiplication with the corresponding ray length l_{ij} (according to Dines and Lytle, 1979; McMechan, 1983) as well as after the treatment of all rays which touch the respective cell N_j times:

$$k_j = \Delta\tau_i \frac{l_{ij}}{\sum_{j=1}^{J} l_{ij}^2} \quad \Rightarrow \quad \bar{k}_j = \frac{1}{N_j} \sum_{j=1}^{J} k_j \tag{9}$$

This process is continued until reaching of a convergence criterion. Thereby, SIRT converges to the least-squares solution (see Ivansson, 1983). The resulting set of area averaged values of slowness and sound velocities, respectively, is called tomogram.
According to Santamarina (1994) the fidelity and quality of inversions are conditioned by the nature of the analysed phenomenon, the quality of measured data and the applied inversion procedure. Errors in the data set can lead to a tomogram with artificial chess board pattern during the iteration cycle, especially, without an averaging process of the corrections k_j. A minimum difference between the measured and simulated data is only the necessary, but not a sufficient condition for the convergence to the correct model. For strongly erroneous data only a solution with a maximum entropy can be found. Furthermore, possible artefacts in the solution can be caused by badly sampled cells and non-ideal ray geometry, especially, for longer rays (Trampert and Leveque, 1990). The larger the distance between source and receiver, the larger is the measuring effect and the influence of the measurement to the tomographic solution. Therefore, the accuracy of the signal and data analyses as well as the positions of the sources and receivers are very important for a successful tomography.
In medical applications it is possible to produce an isotropic and homogeneous ray coverage. For an application in the atmosphere, however, usually both of these properties do not hold. The non-ideal ray distribution can lead to streaks that radiate from anomalous blocks along the direction taken by the rays traversing these blocks. By reducing the weight given rays aligned in common orientations this effect can be reduced (see Humphreys and Clayton, 1988). Only anomalies bordered and crossed by ray paths can accurately be reconstructed, otherwise a smearing of inhomogeneity can occur. Damping, slowness constraints or the use of other prior information effectively removes the possible problems due to the underdetermination of the system of equations (see Bregman et al., 1989; Krajewski et al., 1989). Therefore, we have also to deal with these topics to improve our tomographic results in the future.

4. Numerical modelling of the sound propagation and travel time tomography

Under special conditions, given in chapter 2, the sound propagation through the atmosphere can be described with a ray-tracing model. In the presented study a two-dimensional (x-z) ray-tracing model for a homogeneous atmosphere in the horizontal direction is applied to determine the principal characteristics of sound propagation in the atmosphere and the difference between a straight and curved ray according to actual conditions. It is assumed in our model that the sound propagation follows the x-direction (see Raabe et al., 1996) in a Cartesian coordinates system. The atmosphere is thereby divided into height levels with thickness, Δz. Equation (4) and the relations

$$\Delta s = \sqrt{\Delta x^2 + \Delta z^2}$$

$$\Delta x = \Delta z \cdot \tan\alpha_2 = \Delta z \frac{\sin\alpha_2}{\sqrt{1-\sin^2\alpha_2}} \qquad (10)$$

are used for the calculation of the ray path Δs inside the vertical and horizontal range Δz and Δx, respectively. Vertical temperature and wind profiles from a numerical atmospheric boundary layer model (see, e.g., Mix et al., 1994; Ziemann, 1998) with high resolution of a few centimetres in the lowest 20 m or from experiments, i.e., from a meteorological mast, are used as start values for the ray-tracing model.
The discrepancies between the actual calculated ray path, which is influenced by the angle of emission, and the exactly straight ray path between the source and the receiver amount to

about 0.20 m for a source-receiver-distance of about 200 m (see Figure 2). This value nearly agrees with the results obtained by Spiesberger and Fristrup (1990) for a linear profile of the sound speed under typical daytime conditions.

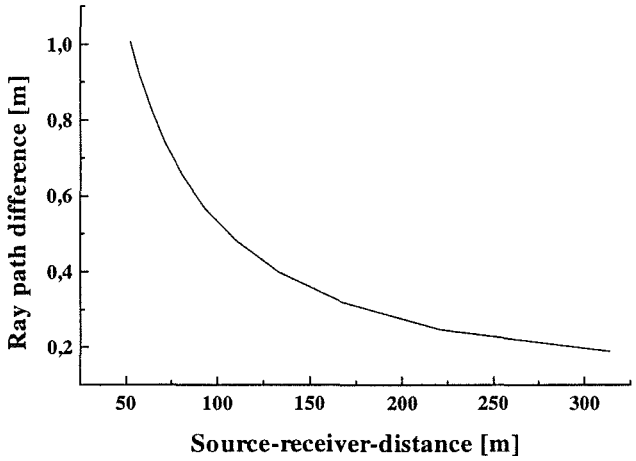

Fig. 2. Differences between the actually calculated ray path from the ray tracing model and the exactly straight ray path between the source and the receiver in dependence of the source-receiver distance using measured temperature and wind data from the 25th of October 1997, 10.00 MET (downwind conditions).

Up to now area averaged values can be considered by a straight ray two-dimensional (x-y) tomographic model. Therefore, the influence of the curved ray path in the vertical direction has to be estimated with the ray-tracing model. The basic set of equations used in the tomographic model was already explained in the previous chapter.

One disadvantage of the presented SIRT is that information about the resolution matrix, according to Backus and Gilbert (1968), is not available. A quantitative measure of the similarity of the reconstructed image and the model is defined by the Euclidic distance (ED) with the actual model-slowness, s_k, and the current estimate, s_k^n, from the n^{th} iteration cycle (see Krajewski et al., 1989)

$$ED = \frac{1}{K} \sum_{k=1}^{K} (s_k - s_k^n)^2 . \qquad (11)$$

It is obvious that the inversion result becomes better for smaller than for larger ED.

To avoid the divergence of the solution and the formation of artefacts due to erroneous data, the number of iterations should be limited corresponding to the optimal reconstruction result. Therefore, the sum of squared residuals (SSR) from equation (9) is a quantity describing the progress of the solution of the equation system. The optimal image will be achieved if the current decrease of SSR-values, averaged over five iteration cycles, diminishes to about 1% of the decrease during the first five steps (see Krajewski et al., 1989). In our study this value is reached not later than after 100 iterations taking a computational time of about one minute on a PC (Pentium 100 MHz).

The size of the grid cells (see Fig. 1) has to be chosen that on one hand area elements are crossed by a relatively great number of rays and on the other hand the wished resolution for searched distribution of meteorological parameters is achieved. The spatial resolution depends on the ray density, grid-spacing and travel time precision. The better the measured travel times and the greater the amount of the temperature inhomogeneity are, the smaller is the anomaly size which could be resolved. The size of the grid cells has to be chosen according to a Krajewski et al (1989) about one times the minimum dimension of resolvable anomaly.

Because of the actual measuring arrangement not all grid cells are passed through with a sufficiently high number of sound rays. The empty places are filled up with additional values for fictitious sources and receivers from geometrical relations between them. Thereby, two travel time measurements are the starting-points. Additional values are calculated for imaginary sources and receivers between the real ones using the averaged travel time data for fictional ray paths.

5. Experimental procedure and data analyses

The experimental studies should give an answer to the following questions:

(1) Which solution is attainable to estimate meteorological parameters and which additional information is necessary?

(2) Is there a possibility of producing absolute data (temperature and wind field) in contrast to Spiesberger and Fristrup (1990) and Wilson and Thomson (1994), or only fluctuations to a known initial state?

To obtain meteorological relevant data (temperature $\pm$ 0.3 K, wind velocity $\pm$ 0.5 ms^{-1}) a lot of requirements are obligatory.

The demanded accuracy for the travel time measurements can derived in similar manner like Spiesberger and Fristrup (1990). The travel time difference between the actual travel time τ_1 along ray path Γ_1 and the undisturbed, that means without wind influence, reference travel time τ_0 along the ray path Γ_0 is given by:

$$\tau_1 - \tau_0 = \int_{\Gamma_1} \frac{dl}{c_1(\Gamma_1) + \vec{u}(\Gamma_1)\cdot\vec{l}} - \int_{\Gamma_0} \frac{dl}{c_0(\Gamma_0)}, \tag{12}$$

where $\vec{u}$ is the wind vector, $\vec{l}$ is the unit vector along the ray path, dl is the differential length of the path and c_0 and c_1 are the sound velocities. Thereby, it will be assumed that $c_1 = c_0 + \delta c$. Assuming approximately equal ray paths leads to:

$$\tau_1 - \tau_0 = \int_{\Gamma_0} - \frac{dl(\delta c + \vec{u}\cdot\vec{l})}{c_0^2 + c_0\delta c + c_0(\vec{u}\circ\vec{l})}. \tag{13}$$

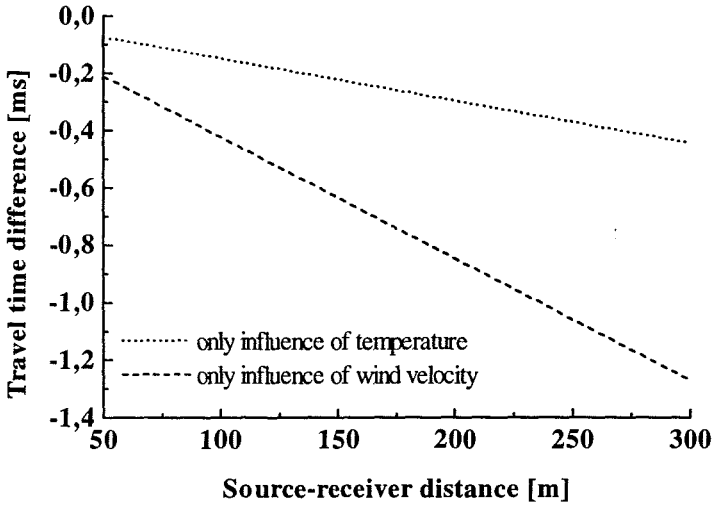

Fig. 3. Demanded travel time accuracy corresponding to only an influence of air temperature (air temperature: 15°C, wished accuracy: 0,3 K) and only a wind influence (wind velocity: 0,5 ms^{-1}, wished accuracy: 0,5 ms^{-1}) for source-receiver distances of the experimental campaign MEPEX'97.

Figure 3 illustrates the great influence of the source-receiver distance for the demanded travel time accuracy computed with equation (13) corresponding to temperature influence without wind on one side and with wind influence without temperature changes on the other side.
The travel time measurements have to be carried out with a high degree of accuracy. This includes, as pointed out already, the precise determination of the distance between source and receiver, the synchronisation of all connected instrumentation and the data processing. Additionally, the separation of different effects on travel time is necessary. A single travel time measurement contains mixed information on temperature and the component of wind along the path. With the rough approximation of a reciprocal sound propagation (straight rays) along the same path a separation of the two effects for a first view is possible.
In cooperation with the Instiute for Tropospheric Research (IfT) Leipzig an experimental campaign was carried out on a grassland site near Melpitz, 50 km north east of Leipzig. Besides several surface layer flux measurements, carried out by IfT, the essential aim for the field experiment was to check the acoustical system developed at our Institute for Meteorology.
Figure 2 shows the layout of the tomographic array of 260×200 m^2. Six sources, compression drivers and four receivers were positioned on tripods at a height of 2 m and 4.5 m, respectively (see Fig. 4 and 5).

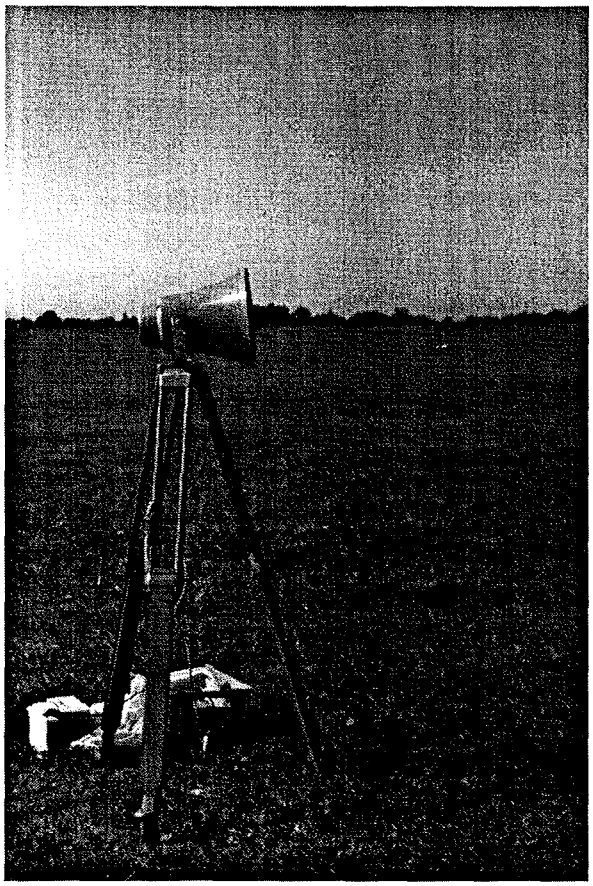

Fig. 4. The speaker system (compression driver, amplifier, portable battery supply).

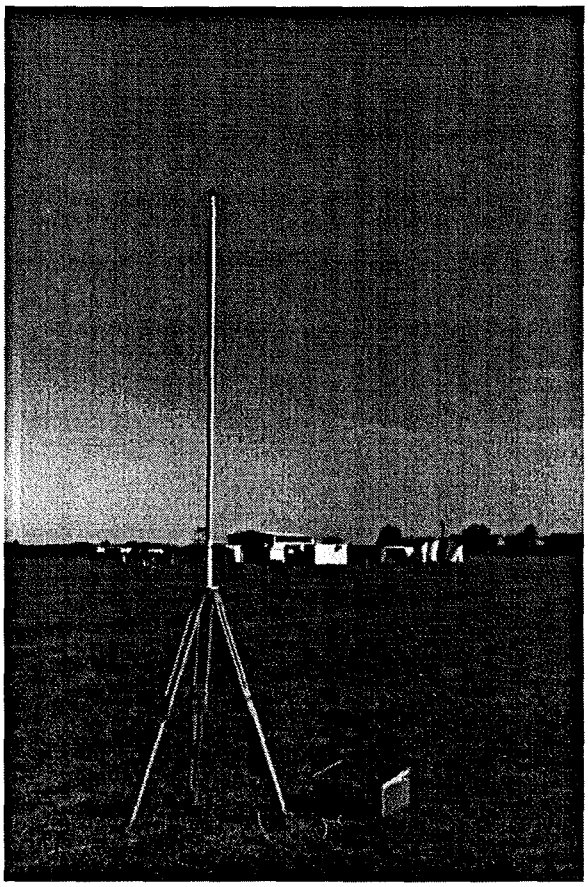

Fig. 5. One receiver set (microphone at a prolonged tripod and a data logger).

The positions of the transducers were determined using trigonometric measurements with an accuracy of 0.1 cm. The effects of the extension of the technical device (speaker: ± 10 cm, mi-

crophone ± 1 cm) can be neglected during the post processing calculations. In different short distances (between 3 m and 10 m) the transmitted signal was recorded and from the shift of a marked point the influence of the speaker extension can be estimated.
All sources simultaneously transmit an acoustic signal. The signal is a sine oscillation with a double peak with a duration in each case of 4 ms, however, the ringing of the compression driver prolongs the signal (see Fig. 6).

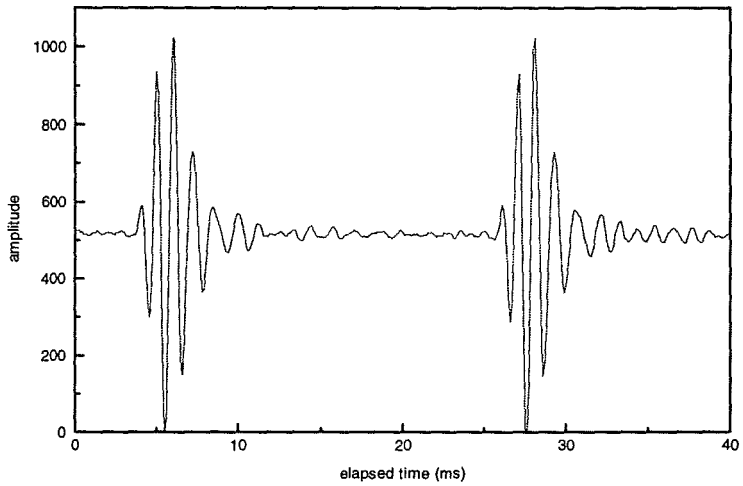

Fig. 6. Example of the transmitted signal: sine oscillation with a double peak (duration of 4 ms) with a constant frequency of 1000 Hz.

Using this special signature at unsatisfactory signal/noise ratios a clear identification of the transmitted signal is possible. The duration of the signal was chosen to be very short to prevent overlapping of different signals. Although the function generator can provide any frequency can be chosen, mostly a constant frequency of 1000 Hz was used. The function generator is additionally connected with all data loggers and gives the start signal for registration. So synchronisation of all devices is ensured.
A receiver set consists of an one inch microphone, a sound level meter and a data logger. The sound level meter is used for power supply and band-pass filtering. After amplifying the signals were sent to the A/D converter. The 10 Bit converter was capable of sampling at a rate of 10 kHz. The digitised data were immediately transferred in a circular system to a hard drive (laptop) that collects all recorded data. So an expensive solution with several memory cards is not necessary.
The travel time of each signal was estimated from the recorded data by cross correlation between the received (output) and the transmitted (input) signal. Each peak of the cross correlation is associated with a separate ray path. The delay time corresponds to the travel time of the transmitted signal. Using the input signal as an calibration signal all delays caused by the device can be eliminated. Figure 7 and Figure 8 show an example of the recorded signals and the cross correlation of the filtered signal with the reference signal. Figure 8 indicates the satisfying signal/noise ratio for all distances.

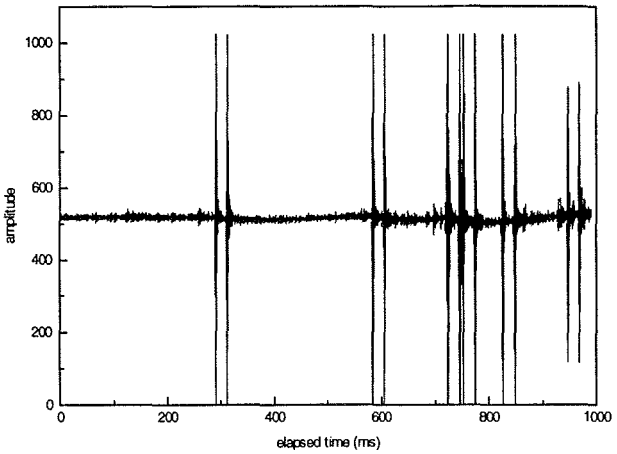

Fig. 7. Example of recorded signals (Receiver R3) after bandpass filtering during the tomography experiment on the 17th of September 1997, 13.02 MET.

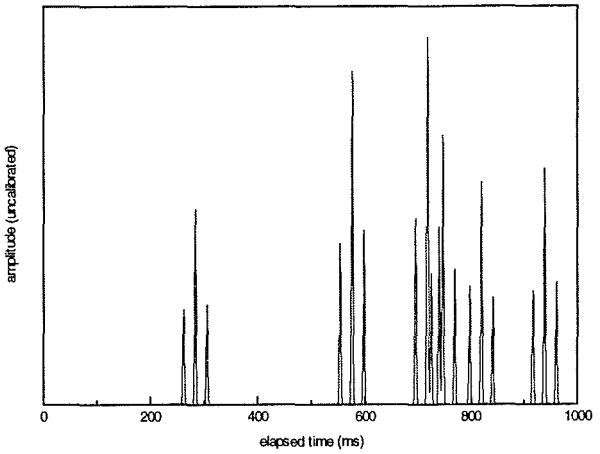

Fig. 8. Cross correlation of the filtered signal (Fig. 7) with the reference signal.

The assignment of each signal to the corresponding source is possible taking the tomographic array layout where all single rays have significantly different path lengths.
The effect of ground reflection can be roughly estimated from a simple geometrical travel time difference between the direct and the reflected sound ray according to Klug (1991). The larger the source-receiver distance is, the smaller the path and travel time difference will be. In this case the travel times can only be distinguished using an information about the amplitude which is smaller for the ground reflected ray over grassland than that without such reflection.
To simulate the actually sound propagation in the atmospheric surface layer the data from the meteorological mast at the Melpitz site were used as aforementioned. The mast (12 m high) is instrumentated with 8 cup anemometers, 8 temperature sensors and one wind-vane.
Additionally, measurements of wind and temperature, which are accomplished with two ultrasonic anemometers, were used for the validation of the tomographic model and to compare the area averaged data with point measurements.

6. First results

Area averages of the effective sound velocity, with one value for each grid cell, were calculated with the travel time data from the introduced experimental campaign (see Fig. 9).
Although the obtained values are not yet recalculated into meteorological parameters principal temperature trends are visible. The heating phase on the 25th of October, a so called 'golden day', is reproduced through increased values of the sound speed. Another interesting effect is the cold edge on the upper right side of Fig. 9 in both parts. It is presumable caused by the cooling power of a water ditch. This indicates that, it is possible to apply the presented tomographic method to detect inhomogeneities in the landscape, especially, during meteorological field experiments. In the future the area averaged values for sound speed can yield corresponding values for air temperature and wind velocity after a more detailed data analysis.

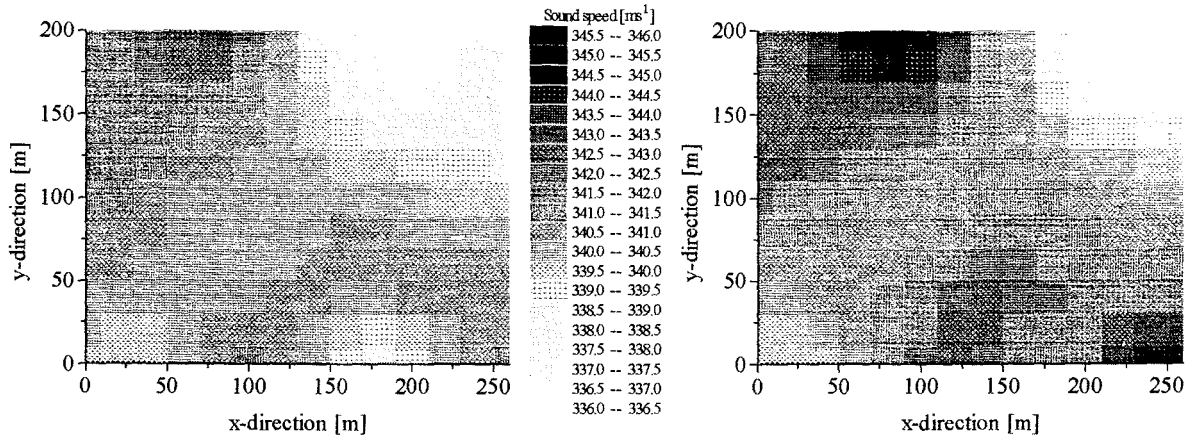

Fig. 9. Area averaged values (one constant for each grid cell) of the effective sound speed as derived from the acoustic travel time tomography for 25th of October 1997.
Left: 10.00 MET, Right: 13.00 MET

7. Conclusions and Outlook

The only small evaluation demonstrates the general applicability of the tomographic monitoring. Acoustic measurements alone are not sufficient for tomographic studies presented. Additional information about wind and temperature profiles are necessary to simulate the general sound propagation in the atmospheric surface layer under different meteorological conditions and to validate the tomographic data.
For meteorological relevant data a higher precision of the procedure is inevitable. Area averages of sound speed can be converted with sufficient accuracy into meteorological parameters, i.e., 0.3 K for temperature and 0.5 ms^{-1} for wind velocity. However, the following improvements are indispensable: a further upgrade of the measuring configuration, a possibility for the exact calculation of the wind influence on the travel time measurements, the use of more traces between receivers to increase the accuracy of travel time determination and also an enlarged number of sources and receivers to obtain a better area coverage.
Up to now only a straightforward sound propagation and area averaged values can be considered with a two-dimensional (x-y) tomographic model. Therefore, improvements with regard to an expansion in the vertical model direction have to be applied in order to get volume averaged values of meteorological parameters. Such volume averaged values are usually provided by microscale and LES models which are to be validated by the method developed here.

Acknowledgements

We would like to thank F. Weiße and M. Engelhorn for their support in the development and manufacturing of the measuring system. Furthermore, we, especially, acknowledge U. Teichmann and the staff of the test site Melpitz for the supply of the meteorological data during the field experiment MEPEX'97. We also wish to express our thanks to E. Danckwardt from the Institute of Geophysics at the University Leipzig for the support when adapting the tomographic model to the atmosphere. Thanks also to N. Mölders for fruitful discussions. We also thank the students from the Institute of Meteorology for their assistance during the experiment. This work was supported by the Deutsche Forschungsgemeinschaft under grant Ra 569/3-1.

References

Aki, K. and Richards, P.: 1980, Quantitative seismology-Theory and methods, Vol. II, W.H. Freeman & Co..

Aubry, M., Baudin, F., Weill, A. and Rainteau, P.:1974, Measurements of the total attenuation of acoustic waves in the turbulent atmosphere, J. Geophys. Res., 79, 5598-5606.

Backus, G. and Gilbert, F.: 1968, The resolving power of gross earth data, Geophys. J., 16, 169-205.

Bass H.E.: 1981, Absorption of sound in air: High temperature predictions, J. Acoust. Soc. Am, 69, 124-138.

Birkhoff, G.: 1988, The consistency of models of sound waves in fluids, In: Lee, D. Sternberg, R.L. and Schultz, M.H. (eds.)., Computational Acoustics, Wave propagation, Elsevier Science Publishers B.V., 117-156.

Bolen, L.N. and Bass, H.E.: 1981, Effects of ground cover on the propagation of sound through the atmosphere, J. Acoust. Soc. Am., 69, 950-955.

Bregman, N.D., Chapman, C.H. and Bailey, R.C.: 1989, Travel time and amplitude analysis in seismic tomography, J. Geophys. Res., 94, 7577-7587.

Chessel, C.I: 1977, Propagation of noise along a finite impedance boundary, J. Acoust. Soc. Am., 62, 825-834.

Daigle, G.A., Piercy, J.E. and Embleton, T.F.W.: 1978, Effects of atmospheric turbulence on the interference of sound waves near a hard boundary, J. Acoust. Soc. Am., 64.

Dines, K.A. and Lytle, R.J: 1979, Computerised geophysical tomography, Proceedings of IEEE, 67, 1065-1078.

Embleton, T.F.W., Piercy, J.E. and Olson, N.: 1976, Outdoor sound propagation over ground of finite impedance, J. Acoust. Soc. Am., 59, 267-277.

Fasold, W., Kraak, W. und Schirmer, W. (eds): 1984, Taschenbuch der Akustik, Teil 1, VEB Verlag Technik, Berlin.

Gilbert, P: 1972, Iterative methods for the three-dimensional reconstruction of an object from projections, J. Theor. Biol., 36, 105-117.

Gordon, R., Bender, R. and Herman, G.T.: 1970, Algebraic reconstruction techniques for three-dimensional electron microscopy and X-ray photography, J. Theor. Biol., 29, 471-481.

Humphreys, E. and Clayton, R.W.: 1988, Adaptation of back projection tomography to seismic travel time problems, J. Geophys. Res., 93, 1073-1085.

Ivansson, S.: 1983, Remark on earlier proposed iterative tomographic algorithm, Geophys. J., 75, 855-860.

Klug, H.: 1991, Sound-speed profiles determined from outdoor sound propagation measurements, J. Acoust. Soc. Am., 90, 475-481.

Kneser, H.O.: 1961, Schallabsorption und -dispersion in Gasen, 192-195, In: Handbuch der Physik, Band XI/1, Springer-Verlag, Berlin.

Krajewski, C., Dresen, L., Gelbke, C. and Rüter, H.: 1989, Iterative tomographic methods to locate seismic low-velocity anomalies: A model study, Geophys. Prosp., 37, 717-751.

McMechan, G.A.: 1983, Seismic tomography in boreholes, Geophys. J. R. astr. Soc., 74, 601-612.

Mix, W., Goldberg, V. and Bernhardt, K.-H.: 1994, Numerical experiments with different approaches for boundary layer modeling under large-area forest canopy conditions, Meteorol. Z., N.F. 3, 187-192.

Munk, W.H., Worcester, P. and Wunsch, C.: 1995, Ocean acoustic tomography, Cambridge University Press, New York.

Peterson, J.E., Paulsson, B.N.P. and McEvilly, T.V.: 1985, Applications of algebraic reconstruction techniques to crosshole seismic data, Geophysics, 50, 1566-1580.

Pierce, A.D.: 1989, Acoustics. An introduction to its physical principles and applications, Acoustic. Soc. Am., New York.

Raabe, A., Arnold, K. and Ziemann, A.: 1996, Akustische Tomographie im Bereich der Atmosphärischen Grenzschicht, Wiss. Mitt. Inst. für Meteorol. Univ. Leipzig und Inst. für Troposphärenforschg. Leipzig, 4, 113-123.

Radon, J.: 1917, Über die Bestimmung von Funktionen durch die Integralwerte längs gewisser Mannigfaltigkeiten, Berichte Sächs. Akademie der Wiss., 69, 262-277.

Rasmussen, K.B.: 1986, Outdoor sound propagation under the influence of wind and temperature gradients, J. Sound Vibr., 104, 321-335.

Rüter, H. and Gelbke, C.: 1986, Seismische Tomographie, In: Dresen, L., Fertig, J., Rüter, H. and Budach, W. (ed.): 6. Minitrop-Seminar. Seismik auf neuen Wegen. Ausgewählte Beispiele und Schwerpunkte, DVGI-Fachauschuß Geophysik Celle, 207-240.

Salomons, E.M.: 1994, Diffraction by a screen in downwind sound propagation, A parabolic-equation approach, J. Acoust. Soc. Am., 95, 3109.

Santamarina, J.C. and Reed, A.C.: 1994, Ray tomography: errors and error functions, J. Appl. Geophys., 32, 347-355.

van der Sluis, A. and van der Vorst, H.A.: 1987, Numerical solution of large, sparse linear algebraic systems arising from tomographic problems, In: Nolet, G. (ed.), Seismic tomography, D. Reidel, Dordrecht, 49-83.

Spiesberger, J.L. and Fristrup, K.M.: 1990, Passive localization of calling animals and sensing of their acoustic environment using acoustic tomography, Am. Natural., 135, 107-153.

Tatarskii, V.I.: 1961, Wave propagation in a turbulent medium, McGraw-Hill Book Company, New York.

Trampert, J. and Leveque, J.-J.: 1990, Simultaneous iterative reconstruction technique: Physical interpretation based on the generalized least squares solution, J. Geophys. Res., 95, 12553-12559.

Wilson, D.K. and Thomson, D.W.: 1994, Acoustic tomographic monitoring of the atmospheric surface layer, J. Atm. Ocean. Technol., 11, 751-768.

Worthington, M.H.: 1984, An introduction to geophysical tomography, First Break, 2, 20-26.

Ziemann, A., 1998: Numerical simulation of meteorological quantities in and above forest canopies, Meteorol. Z., accepted.

Address of Authors:

Astrid Ziemann, Klaus Arnold, Dr. Armin Raabe
Institut für Meteorologie
Universität Leipzig
Stephanstr. 3
D-04103 Leipzig